Ceramic Plugs for Deep Borehole Seals – 17316

William Lowry *, Ken Coates *, Ken Wohletz *, Sandra Dunn *, Andrew Duguid **, Bill Arnold ***, Ed Patera, Lori Groven ****
* Olympic Research, Inc.
** Battelle
*** Arnold Hydrogeology Consulting
**** South Dakota School of Mines and Technology

ABSTRACT
In the deep borehole nuclear waste disposal concept, waste packages are emplaced deep in crystalline rock formations under conditions of high pressures, high mineral content water, and elevated temperatures. Well seals and plugs must perform for thousands of years. A novel ceramic plug system under development capitalizes on the thermal energy of thermite mixtures and engineered additives to react and form ceramic-like plugs in place with favorable structural, flow, and geochemical properties. Depending on the ingredients, the reaction can produce aluminosilicates, plagioclase feldspars, or other combinations in crystalline or amorphous forms. Normative mineralogy techniques were applied to predict product mineralogy and evaluate compatibility with host rocks, and showed they are comparable to igneous rock analogs. The results support a tentative geochemical compatibility between these formulations and granitic host rock. Because the reaction produces a significant amount of thermal energy, the thermal/structural/fluid response of the plug and surrounding media was evaluated with the FEHM code. Temperatures near the plug/rock interface are estimated to peak at less than 600°C and cool to near ambient temperature within a day. Rock stresses resulting from the thermal pulse are predicted to be similar to the unconfined compressive strength of granites, and generally lower than triaxial test results. Entrained fluid expansion due to heating was shown to be lower than failure stresses. Little or no failure in the surrounding media would be expected due to the plug formation process. The present efforts are focused on refining the material formulations, evaluating the geochemical and mechanical interactions between the plug and host rock, and testing the plug formation process in scaled granite and basalt masses.

INTRODUCTION
Deep borehole disposal of nuclear waste is considered an alternative to geologic repositories for long term disposition of spent nuclear fuel, sealed sources, and high level waste forms. In this concept, boreholes would be drilled in deep crystalline rock to depths of 3 to 5 km, waste packages emplaced in the lower 2 km of the borehole, and backfilled with a combination of plug and granular backfill materials. The water at these disposal depths is dense due to its high mineral content, and is relatively immobile, resulting in inherent isolation from the biosphere.

The reference design for the disposal scenario [1] places waste packages in the lower, uncased region of the borehole. The borehole is filled with a combination of

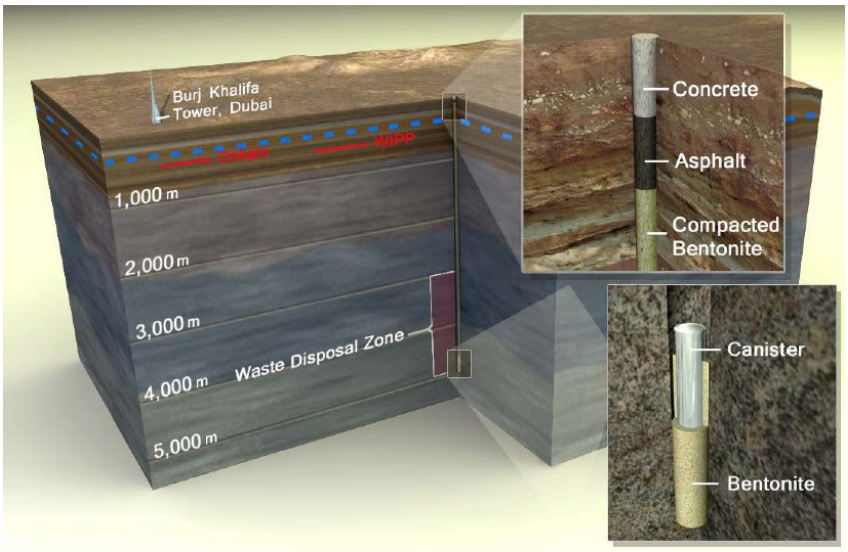

Figure 1. Generalized concept for deep borehole disposal of high-level waste [1]

bentonite sealing plugs, cement and asphalt structural plugs, and granular material, as shown in Figure 1. Plugs are critical features of the system design. They serve as platforms to bear the backfill column load and as low permeability seals. The high hydrostatic and lithostatic pressures, high salinity, and high temperature due to the geothermal gradient pose engineering challenges to the long term performance of traditional cement and granular plug methods.

The ceramic plug system forms very strong, geochemically stable, and low permeability features in place using the Self-propagating High-temperature Synthesis (SHS) process. This approach capitalizes on the energy released from solid metal/oxide exothermic reactions to form various types of ceramic-like materials. The aluminum and Fe_2O_3 (ferric oxide) thermite system is used due to its favorable product characteristics, energy density, and ready availability. The reaction for this system is:

$$Fe_2O_3 + 2Al \rightarrow Al_2O_3 + 2Fe + \text{Heat (3956 J/g)}$$

Aluminothermite systems are attractive in these applications because a major constituent of the reaction product is aluminum oxide. With careful selection of diluent materials, the reaction characteristics (reaction rate, stability, and peak temperature) can be controlled and final products developed ranging from aluminosilicates to feldspar minerals, in crystalline and amorphous forms. In typical formulations, the iron product will settle out and form a solid mass at the base, leaving a nearly pure, low porosity ceramic matrix in the upper majority of the plug. Laboratory-prepared samples of these formulations have shown favorable properties:

- Permeability to air flow as low as 1 μDarcy
- Unconfined compressive strength: 47 to 210 MPa
- Young's modulus: 15 to 111 GPa

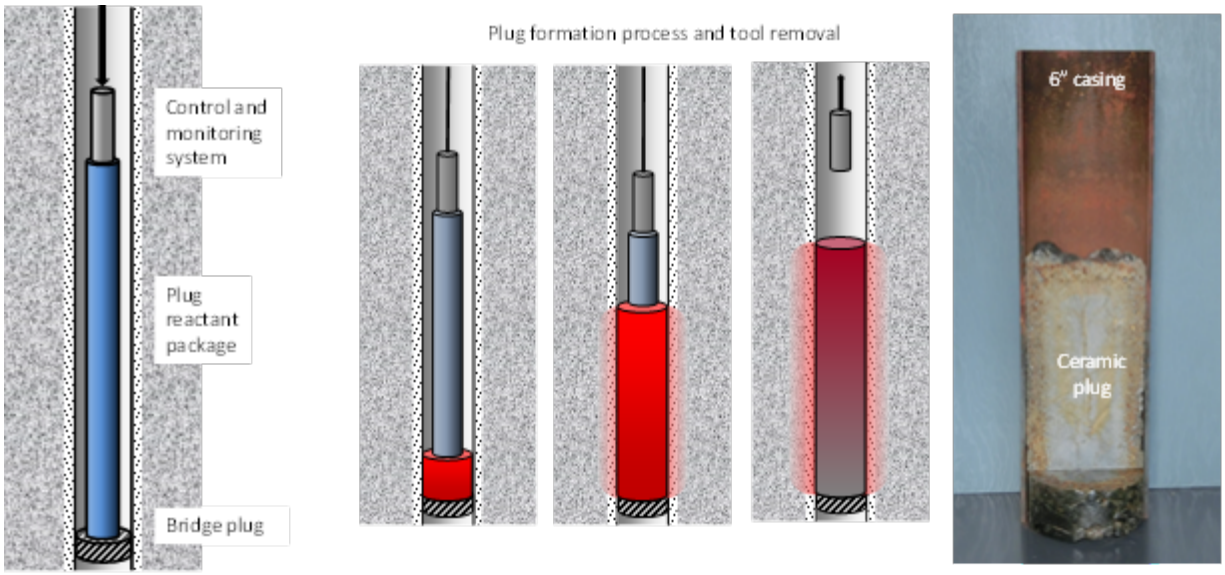

Figure 2. Ceramic plug emplacement process, and example product form in cased experiment.

The plug emplacement process and example test plug formed in dry conditions are shown in Figure 2. The downhole package, consisting of the thermal charge and its ignition system, is assembled at the wellhead. Electrical and mechanical interfaces are connected, and the package lowered into the well via a wireline system. At the target depth, the package rests on a platform (mechanical bridge plug, cement, or granular backfill). The package is ignited at the base of the charge, and the weight of the charge compacts the reacted material into the well volume as the reaction progresses up the charge. When the charge reacts to the top of the charge package, its mechanical link to the top load is consumed and released. The control package is then retrieved to the top of the well.

METHODS

The ceramic plug material can be characterized as a self-forming 'synthetic rock' seal. In the following sections the composition of reaction products is evaluated, and the impact of its released thermal energy on the surrounding media predicted.

Normative mineralogy

Thermite/additive mixtures, tested as plug materials for lined and unlined boreholes, were analyzed by their normative mineralogy in comparison to igneous rock analogs (such as granite, monzo-gabbro, and syenite). The most notable differences between these thermite mixtures and granite analogs are the higher abundance of iron phases and lower abundance of silica in the mixtures, even though the analogs range from slightly undersaturated to oversaturated with respect to silica. Normative mineralogy also predicts densities near those of granite at 2.6-2.8 Mg/m^3, liquidus temperatures from 1200-1500 °C, and viscosities around 10^1 - 10^4 Pa-s at 1000°C and 10^{-2} – 10^{-1} Pa-s at 1500°C. These results support a tentative geochemical compatibility between these plugs and granitic host rocks

and show that predicting mineralogy may have utility for tailoring thermite mixtures for specific applications where both geochemical stability and fluid properties need to be optimized.

Plug materials systems considered in this study are formed by combining aluminothermite (an aluminum/iron oxide thermite) with additives designed to moderate the reaction, control its peak temperature, and form products with specific fluid and solid mechanical and geochemical properties. The basic thermite reaction yields native iron and aluminum oxide. The additives may consist of metal oxides, minerals, or glasses, depending on the desired end product. Addition of SiO_2, for example, can yield an aluminosilicate crystalline product such as mullite, which forms a ceramic matrix. Other additives, like tectosilicates or inosilicates minerals, will combine with the reaction products to produce solid solution systems such as the anorthite/albite system. Glasses are added to produce an amorphous matrix with a low solidification temperature, useful when conformance to steel surface casing is desired.

Because of the use of silicate additives the plug mimics naturally occurring igneous rocks. Therefore, a useful way to evaluate experimental plug compositions is to analyze their silicate rock affinities, modeling them as igneous rock analogs. This analysis can be accomplished by a normative mineralogy calculation (known as *CIPW*; Cross et al. [2]; Kelsey, [3]) that models idealized mineralogy of rocks. It is especially useful for very fine-grained and glassy rocks for which modal mineralogy is difficult to quantify. The normative mineralogy of the rock is calculated, based upon assumptions about the order of mineral formation, known phase relationships of minerals, and simplified mineral formulas. The calculated mineralogy can be used to assess rock forming concepts such as silica saturation, aluminosity (balance among aluminum oxide and oxides of calcium, sodium, and potassium), mineral paragenesis (sequence of crystallization with quenching), and geochemical stability with respect to crystalline rocks in the environment of application.

We apply the KWare Magma software for the normative calculation. This software also provides igneous rock classifications endorsed by the IUGS (International Union of Geological Sciences; *e.g.*, Le Bas and Streckeisen, [4]; Le Maitre et al., [5]; Cox et al., [6]), and it applies a mixing model for multicomponent rock systems that approximate liquidus temperatures and temperature-dependent densities and viscosities. These calculations are based on the methods of Bottinga and Weill [7,8] and Shaw [9], who apply adaptations of the Arrhenius mixture rule over a wide range temperatures and compositions by calibration with experiments with synthetic mixtures.

Among a large number of tested mixes, the following (Table1) are examples of five types.

- C1 – This mix produces a predominantly anorthite (calcium feldspar) product
- C2 – Higher dilution anorthite product with albite (sodium feldspar) and glass added to lower melt temperature and viscosity
- C3 – Albite/glass diluent, which produces an amorphous, predominantly albite product

- C4 – Pure silica diluent, resulting in an aluminosilicate (mullite) product
- C5 – MnO_2 thermite system diluted with silica and glass

Table 1.Experimental Mixtures (mass fractions)

Constituent	C1	C2	C3	C4	C5
Al	0.176	0.151	0.177	0.177	0.157
Fe_2O_3	0.523	0.449	0.523	0.523	0.417
$NaAlSi_3O_8$	0.00	0.044	0.25	0.00	0.00
SiO_2	0.085	0.136	0.00	0.30	0.23
MnO_2	0.00	0.000	0.00	0.00	0.076
Glass	0.053	0.044	0.05	0.00	0.12
$CaSiO_3$	0.163	0.176			0
Total	**1.00**	**1.00**	**1.00**	**1.00**	**1.00**

The above mixture constituents required conversion to conventional major element oxide components for calculation of the following mineralogy (Table 2). These results match fairly close to those of quantitative X-ray diffraction (XRD) analyses of homogenized powders of these mixtures: C1--anorthite-rich (An93) rock with accessory corundum and minor nepheline and olivine; C2--anorthite-Albite solid solution (An82-bytownite) with accessory mullite (QZ+CO) and minor hypersthene; C3--albite (An07) with corundum and minor nepheline and olivine; C4--mullite with corundum; and C5--mullite with Oligoclase (An27) and minor hypersthene.

Although mullite is a known phase in some thermite mixtures, it is not included in igneous rock normative compositions because of its relatively rare natural occurrence and phase relationships. As such, where corundum and quartz are predicted normative phases for these mixtures, XRD analyses confirm the two combine as a prediction of mullite. Similarly, hercynite ($FeO+Al_2O_3$) is a spinel not common in igneous rocks, but its presence in normative calculations is predicted by occurrence of corundum and iron oxide.

Table 3 shows the calculated classifications and physical properties for these mixtures, and Figure 3 shows IUGS classifications for coarse-grained (aphanitic/plutonic) igneous rocks for which the upper ternary diagram is for silica-saturated rocks and the lower is for silica undersaturated rocks. Note that all five of the mixtures plot near or above calculated silica saturation. The upper triangle represents the range of granitic rock composition. The lower right corner is where rocks with higher amounts of calcic plagioclase (anorthite, bytownite, laboradorite) plot, and those with abundant Mg-Fe minerals (mafic) are termed *gabbro*. The bulk densities calculated for these mixtures match well with granitic rocks, but the modeled viscosities are better matches for gabbros (basalts) in general.

Table 2.Calculated Normative Mineralogy (weight percentages).

Oxide	C1	C2	C3	C4	C5
Quartz		2.65		25.91	16.89
Corundum	14.59	10.02	27.21	28.88	21.86
Orthoclase					
Albite	2.50	8.49	23.83		12.63
Anorthite	35.75	38.82	1.93		4.77
Leucite					
Nepheline	1.57		1.51		
Diopside					
Hypersthene		0.39			1.06
Acmite					
Wollastonite					
Olivine	0.32		0.30		
Magnetite					18.04
Ilmenite					
Hematite	45.27	39.63	45.23	45.21	24.74
Sphene					
Rutile					
Calcite					

Table 3.Calculated Classification and Physical properties.

	C1	C2	C3	C4	C5
Shand Classification	Peraluminous Silica Undersaturated	Metaluminous Silica Saturated	Peraluminous Silica Undersaturated	Peraluminous Silica Oversaturated	Peraluminous Silica Oversaturated
IUGS Classification	Monzo-Gabbro	Monzo-Gabbro	Syenite	Granite (Monzogranite)	Quartz Monzo-Gabbro
Bulk Density (kg/m^3)	2799	2735	2669	2614	2776
Liquidus (°C)	1540	1453	1453	1223	1367
Viscosity					
1000°C	5-2200	10-9200	1-5200	3-940	2-3500
1250°C	0.29-1.74	0.61-3.95	0.12-1.16	0.19-0.21	0.24-1.93
1500°C	0.01	0.04	0.01	0.02-0.05	0.04-0.07

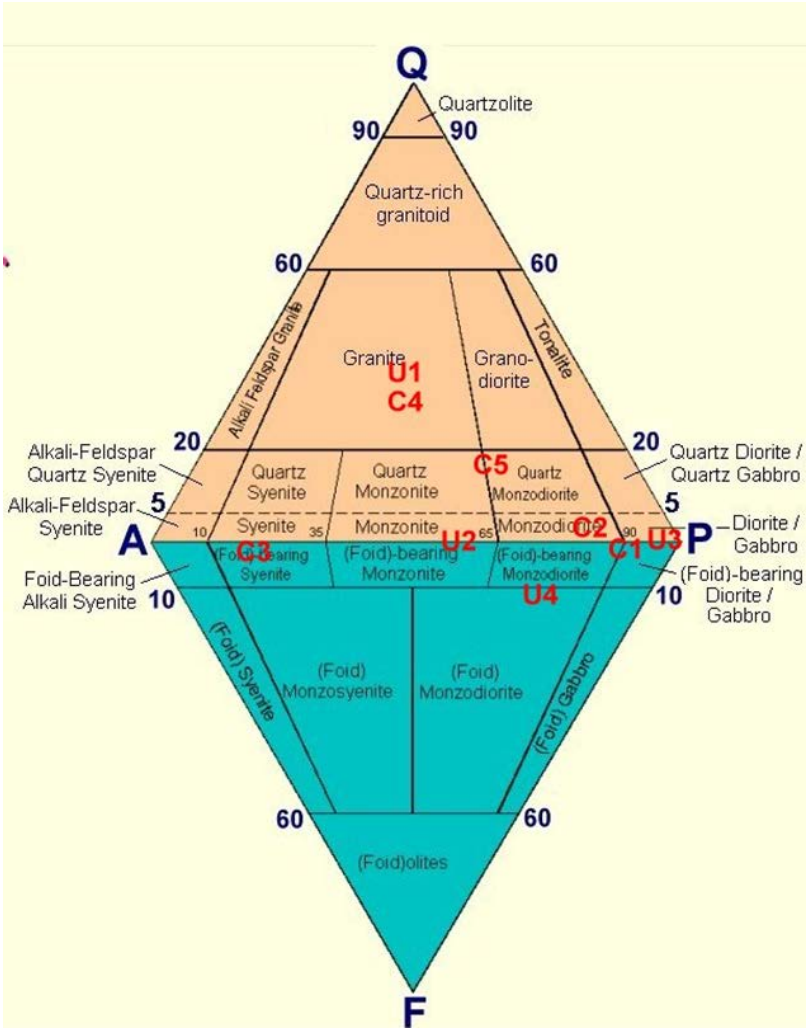

Figure 3. IUGS Classification of aphanitic igneous rocks. Samples C1-C5 and U1-U4 mainly comprise granitic rocks (upper triangle).

This methodology allows prediction of trends in rheological properties as functions of dilution and products, useful for understanding the plug formation process in the well. In figure 4 the predicted viscosity/temperature trends for silica and glass-diluted mixtures depicts viscosity vs temperature, liquidus temperatures, and glass transition temperatures.

Normative mineral calculations show that added silicate diluents, both crystalline and glassy, produce granite analog products that are mostly saturated with silica, enough to form feldspars from soda, lime, and potash added either as minerals or glass. Furthermore the granite analog products are peraluminous (molar proportion of alumina is greater than that of the sum of the calc-alkalic oxides) a situation typical of S-type granites formed from sedimentary protoliths. For uncased borehole applications there is a good degree of chemical compatibility that can ensure

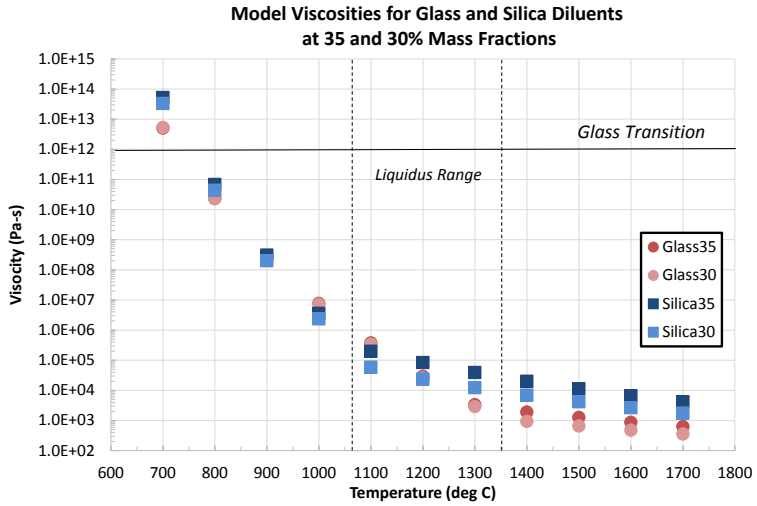

Figure 4. Viscosity/temperature relationships for glass and silica diluted formulations, using the Magma mineralogical model.

prolonged geochemical stability with granitic rocks. These results, combined with XRD, SEM/EDS, and petrographic microscopic characterization, help assess the formation of amorphous and crystalline phases, liquidus temperatures, densities, and viscosities necessary to design plug formulations for specific applications, such as where bonding to steel casing is critical or flowing into borehole irregularities or fractures is desired.

This initial evaluation for thermite with silicate additives leads to the following general conclusions:

- The process forms silicate compositions of crystallized minerals common to granitic rocks.
- Typical mixtures are silica saturated and aluminum oversaturated.
- Plagioclase feldspars, formed by adding glass, albite, and wollastonite, follow the trend where anorthite melts will crystallize at a higher temperature than albite-rich ones.
- Densities range from 2600-2800 kg/m^3, typical of granitic/gabbroic rocks
- Liquidus temperatures range from 1200 to 1500 C
- Viscosities are temperature dependent and vary over several orders of magnitude from less than 1 Pa-s to several thousand Pa-s.

Thermal, fluid, and mechanical response of the host rock to a heat-generating plug

The thermally formed plug system will result in physical changes within the plug and the surrounding bedrock over a relatively short time frame as the plug solidifies and cools. The resulting high temperature, pressure, and stress gradients may impact the physical characteristics of the bedrock adjacent to the seal. Of particular concern are potential mechanical degradation and fracturing of the bedrock that could increase the permeability in the rock near the plug or impact borehole stability.

Thermal-hydrologic-mechanical (THM) modeling of the thermally formed borehole plugging system was conducted with the objectives of 1) estimating the temperatures and fluid pressures in the rock surrounding the borehole, based on an uncased borehole in granite, 2) estimating the spatial and temporal variations in the THM response of the host rock related to the presence of the borehole and the heat introduced by the plug, and 3) making a preliminary assessment of potential mechanical failure and resulting damage to the rock surrounding the borehole from THM effects.

When the maximum principal horizontal stress is significantly higher than the minimum principal horizontal stress, the highest compressive stress at the borehole wall exists at the locations aligned with the direction of the minimum principal horizontal stress. The borehole wall rock can fail at these locations of maximum compressive stress by shear failure if the stresses exceed the compressive strength of the rock, forming borehole breakouts.

The effective stress experienced by the rock around the borehole may also be impacted by thermal and hydrologic processes through thermal-elastic and poroelastic couplings. Higher temperature in the borehole will heat the adjacent rock by conduction, causing thermal expansion and placing additional compressive stress on the rock near the borehole wall. Pressure of fluids in the rock oppose compressive stress and reduce the effective stress on the rock matrix. Difference in fluid pressure in the borehole and pore pressure in the surrounding rock result in an outwardly directed confining stress at the borehole wall and tends to stabilize the borehole wall. A general equation for the maximum effective hoop stress at the borehole wall is given as:

$$\sigma_{\theta\theta} = 3\sigma_{Hmax} - \sigma_{Hmin} - 2P_p - \Delta P - \sigma^{\Delta T} \qquad Eq.1$$

where $\sigma_{\theta\theta}$ is the maximum effective hoop stress at the borehole wall, P_p is the pore pressure, ΔP is the difference in pressure between the borehole fluid and the pore pressure, and $\sigma^{\Delta T}$ is the thermal-mechanical stress induced by borehole heating.

The THM model of the thermally formed borehole plugging system was set up for application in the disposal of radioactive waste in a deep borehole disposal system outlined in Arnold et al. [1]. The borehole is 43 cm in diameter and ambient physical conditions are representative of a depth of 3 km, which is just above the top of the radioactive waste disposal zone in the reference design for the disposal system. The ambient temperature was assumed to be 75 °C and the fluid pressure corresponds to hydrostatic conditions of 32 MPa.

The THM model was implemented with the FEHM software code [10], which has been enhanced to include the equations of state for supercritical water up to 1500 °C. An unstructured grid consisting of 3-D hexahedral elements was used. The

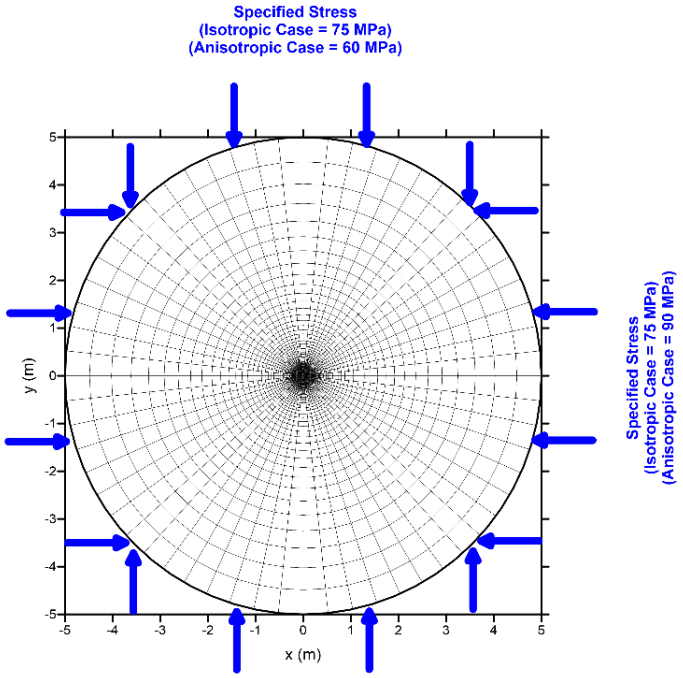

Figure 5. Mechanical boundary conditions applied to the THM model.

initial temperature of the plug is 1500 °C and the lateral mechanical and thermal boundary conditions are shown in Figure 5.

Representative parameter values for granite and the plug are used in the model, as shown in Table 4. Approximate functional relationship for Young's modulus and Poisson's ratio, as shown in Figure 6, were based on data from Saiang and Miskovsky [11] and Wang et al. [12] and applied in the THM model.

Table 4.Parameter values used in the THM model.

Parameter	**Granite**	**Plug**
permeability (m^2)	1.0×10^{-17}	3.0×10^{-17}
porosity (-)	0.01	0.00
thermal conductivity	f(T)	f(T)
density (kg/m^3)	2750.	2560.
specific heat (J/kg K)	800.	1076.
Young's modulus (MPa)	f(T)	f(T)
Poisson's ratio (-)	f(T)	f(T)
volumetric coefficient of thermal expansion (1/K)	24×10^{-6}	0
Biot coefficient	0.3	0.3

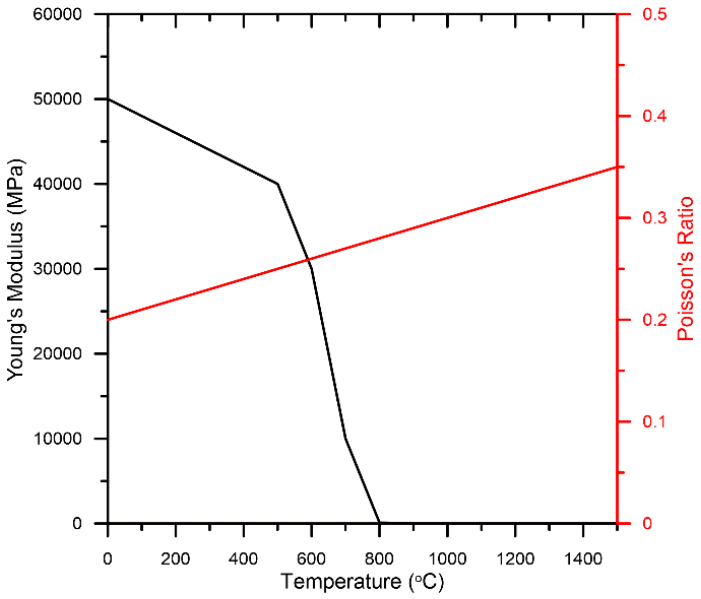

Figure 6. Relationships between Young's modulus, Poisson's ratio, and temperature used in the THM model (granite).

The THM model provides the simulated spatial distribution of state variables such as temperature, pressure, and stress at key times, and time series at specified locations. Figure 7 shows the spatial distribution of the x-direction component of stress at a time of 0.00137 days (about 2 minutes) following ignition of the plug. This time corresponds to the maximum stress at a distance of about 2 cm outside the borehole wall in the direction of the minimum principal horizontal stress (the y-direction), which is the location of maximum hoop stress. The plug has stress values near zero because the value of Young's modulus is very low for the temperatures existing in the plug at this early time.

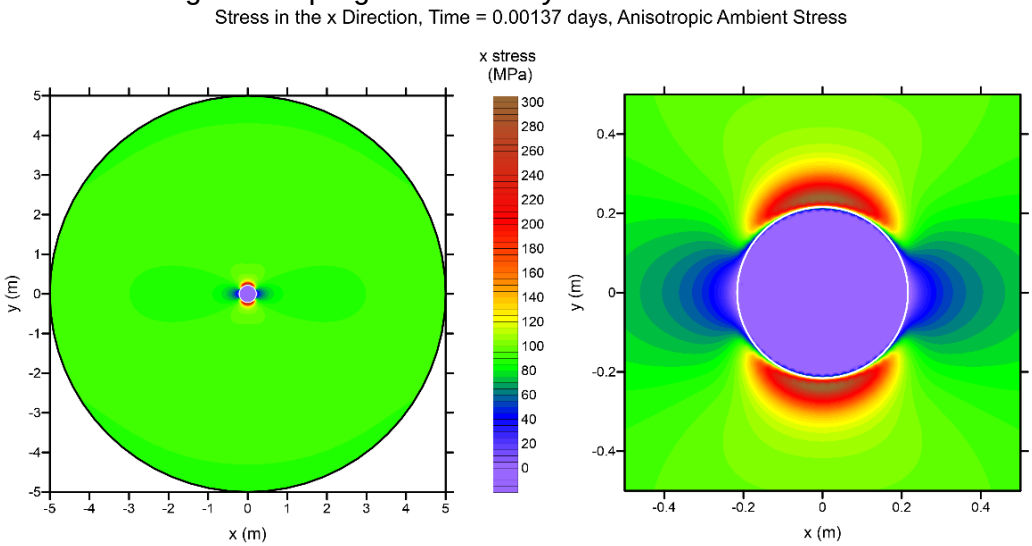

Figure 7. Simulated stress in the x-direction at the time of peak hoop stress in the rock near the borehole wall.

The simulated temperature increases rapidly for the location along the y-axis about 2 cm in the bedrock and reaches a peak value of 561 °C at about 0.0059 days (8.5 minutes) following ignition of the plug and returns to near ambient conditions within one day. The simulated pressure reaches a peak value of 92.6 MPa at about 0.00003 days (2.6 seconds) and declines rapidly within a few hours.

Simulated hoop stress as a function of time is plotted at the location of maximum hoop stress in Figure 8. The total hoop stress, as shown by the dashed line peaks at a value of 317 MPa at a time of 0.00137 days (about 2 minutes). The total hoop stress calculated by the THM model includes the effects of the first, second, and fifth terms on the right side of Equation 1. The effective hoop stress on the granite rock matrix is calculated by subtracting the third and fourth terms on the right side of Equation 1 to account for fluid pore pressure and differential pressure. The simulated effective hoop stress is shown as the solid line in Figure 8, which peaks at a value of 223 MPa at a time of 0.00137 days (about 2 minutes).

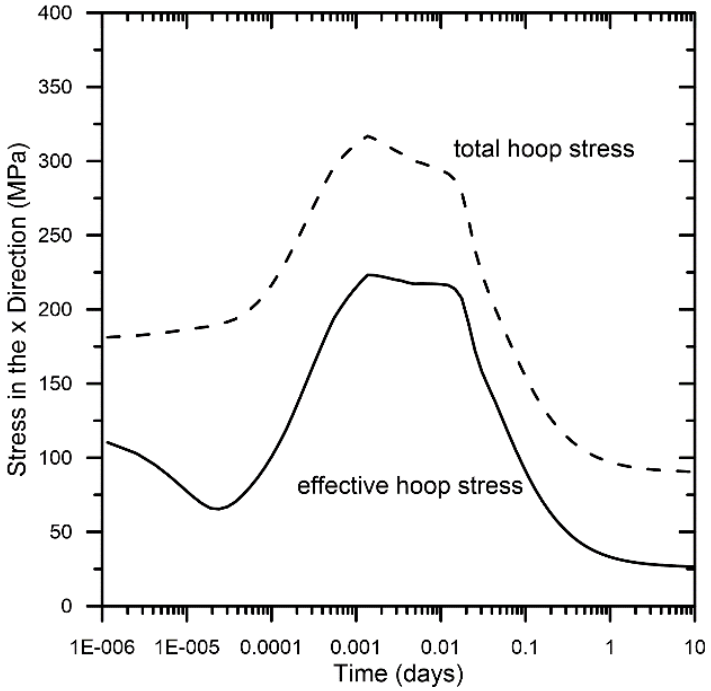

Figure 8. Simulated total and effective hoop stress versus time since plug ignition at the location near the borehole wall in the direction of minimum principal horizontal stress.

As described earlier, one mode of mechanical damage to the host rock and fracturing at the borehole wall is shear failure due to excessive compressive hoop stress. As a preliminary assessment of the potential for such damage from the thermally formed borehole plugging system a comparison is made between the simulated peak effective hoop stress and the compressive strength of granite.

There are limited data on the compressive strength of granite at temperatures higher than room temperature and with significant confining stress. Some additional information is available for samples of granite that have been heat

treated and then retested at room temperature. Data from Wang et al. [12] indicate a general trend of increasing triaxial (confined) compressive strength for granite with increasing temperature (up to 400 °C) and with increasing confining pressure. Most of the data for temperatures between 100 °C and 300 °C for confining stresses of greater than 5 MPa have values of compressive strength of about 240 MPa to 360 MPa. Data from Shao et al. [13] for uniaxial (unconfined) compressive strength tests of medium- and coarse-grained granite indicate decreasing strength with temperature and values of 56 MPa to 161 MPa for experiments between room temperature and 600 °C. The Shao et al. [13] results should be considered as a lower bound for compressive strength because of the unconfined character of the tests. Data from Saiyang and Miskovsky [11] for uniaxial (unconfined) compressive strength tests of granite indicate strengths of about 230 MPa to 240 MPa for samples at room temperature and samples that have been heat treated to 400 °C.

The maximum simulated effective hoop stress near the borehole wall for the thermally formed borehole plugging system is 223 MPa and occurs at a temperature of about 500 °C. This stress exceeds the compressive strength of granite for some of the uniaxial testing data. However, the maximum simulated stress generally does not exceed the compressive strength measurements for triaxial testing under more representative confining stresses (Wang et al., [12]). Overall, comparison of the simulated peak effective hoop stress of 223 MPa with the more relevant lab data (higher confining pressure) suggest that the compressive strength of granite would not be exceeded. It should be noted that considerable variability in mechanical strength likely exists among various types of granite and other crystalline rocks, related to texture, mineralogy, and, foliation.

For these initial simulations of the impact of a plug thermal source in an unlined borehole in crystalline rock, the following conclusions can be drawn:

- Thermal impacts of plug formation on granite borehole wall rock are relatively short lived, but result in temperatures in excess of 500 °C within a few centimeters of the borehole.
- Thermally induced increases in fluid pressure near the borehole peak before the highest temperatures and dissipate quickly.
- Maximum effective hoop stress near the borehole is about 223 MPa and occurs about 2 minutes after plug ignition.
- Comparison with lab data on compressional strength of granite at varying temperatures and confining pressures suggests that intact granite would not be mechanically damaged by the thermal pulse from the plug for the assumed conditions in this modeling. However, maximum effective stress is on the same order as the compressional strength and there is considerable variability in the strength of different crystalline rocks.
- This modeling does not entirely represent the THM behavior of the plug itself because of code and modeling limitations. Such limitations probably do not significantly impact the analysis of behavior in the wall rock, but should be evaluated further.

CONCLUSIONS

Ceramic plugs formed in-situ offer a significant departure from conventional well-sealing methods. The various aluminothermite/additive systems enable a range of product compositions and forms with favorable properties for deep borehole disposal. The plug formation products exhibit very high mechanical strength, low matrix permeability, and inherently high geochemical stability. The normative mineralogical analysis method predicts product composition and key physical characteristics, and suggests that these materials may be very compatible with the crystalline media. The thermal/hydrologic/mechanical analysis showed that thermally-induce pore pressure effects are short-lived and minimal, the induced thermal stresses project only a few centimeters into the rock, are short-lived, and likely will not fail the rock.

The current efforts include a more extensive mineralogical analysis to evaluate plug formation rheology, geochemical stability, and compatibility; refined and expanded thermal analysis to consider more realistic material models for both the rock and plug; and experimental evaluation of plug/rock interactions under a range of applied pressure, scale, and saturation conditions.

REFERENCES

1. Arnold B. W., Brady, P. V., Bauer, S.J., Herrick, C., Pye, S., and Finger, J., Reference Design and Operations for Deep Borehole Disposal of High-Level Radioactive Waste, Sandia national Laboratories, SAND2011-6749, October 2011.

2. Cross W, Iddings J P, Pirrson L V and Washington H S, 1902, A quantitative chemico-mineralogical classification and nomenclature of igneous rocks; J. Geol. 10 555–590.

3. Kelsey C H, 1965, Calculation of the CIPW norm; Mineralogical Magazine 34 276–282.

4. Le Bas, M. J. and Streckeisen, A. L.,1991, The IUGS systematics of igneous rocks. Journal of the Geological Society, London 148, 825–833.

5. Le Maitre, R. W., Bateman, P., Dudek, A., Keller, J., Lameyre, J., Le Bas, M., ... & Woolley, A., 1989, A Classification of Igneous Rocks and Glossary of Terms, Recommendations of the International Union of Geological Sciences, Subcomission on the Systematics of Igneous Rocks. A classification of ingeous rocks and glossary of terms: Recommendations of the International Union of Geological Sciences Subcommission on the Systematics of ingeous rocks.

6. Cox, K.G., Bell, J.D., and Pankhurst, R. J., 1979, The interpretation of igneous rocks, Allen & Unwin, London.

7. Bottinga and Weil, 1970, Densities of silicate liquid systems calculated from partial molar volumes of oxide components, Amer. J. Sci., 269: 169-182

8. Bottinga, Y. A., and Weil, D. F., 1972. The viscosity of magmatic silicate liquids: a model for calculation. Amer. J. Sci., 272: 438-473.

9. Shaw, H. R., 1972. Viscosities of magmatic silicate liquids: an empirical method of prediction. Amer. Jour. Sci. 272: 870-893.

10. Zyvoloski, G.A., 2007, FEHM: A Control Volume Finite Element Code for Simulating Subsurface Multi-Phase Multi-Fluid Heat and Mass Transfer (Report). Los Alamos Unclassified Report LA-UR-07-3359.

11. Saiang, C. and K. Miskovsky, 2012, Effect of heat on the mechanical properties of selected rock types – a laboratory study, Harmonising Rock Engineering and the Environment – Qian & Zhou (eds), © 2012 Taylor & Francis Group, London, ISBN 978-0-415-80444-8.

12. Wang, Yu, Bao-lin Liu, Hai-yan Zhu, Chuan-liang Yan, Zhi-jun Li, and Zhi-qiao Wang, 2014, Thermophysical and mechanical properties of granite and its effects on borehole stability in high temperature and three-dimensional stress, The Scientific World Journal, vol. 2014, Article ID 650683, 11p.

13. Shao, S.S., P.G. Ranjith, and B.K. Chen, 2013, Influence of high temperature on the mechanical behaviour of Australian Strathbogie granites with different grain sizes, 47th US Rock Mechanics / Geomechanics Symposium held in San Francisco, CA, USA, 23-26 June 2013, American Rock Mechanics Association.

ACKNOWLEDGEMENTS

This material is based upon work supported by the U.S. Department of Energy, Office of Science, Office of Nuclear Energy, under Award Number DE-SC0010135.

DISCLAIMER